Eur. Phys. J. B **13**, 369–375 (2000)

THE EUROPEAN PHYSICAL JOURNAL B

EDP Sciences

The link overlap and finite size effects for the 3D Ising spin glass

B. Drossel[a], H. Bokil, M.A. Moore, and A.J. Bray

Theory Group, Department of Physics and Astronomy, University of Manchester, Manchester M13 9PL, UK

Received 25 May 1999

Abstract. We study the link overlap between two replicas of an Ising spin glass in three dimensions using the Migdal-Kadanoff approximation and scaling arguments based on the droplet picture. For moderate system sizes, the distribution of the link overlap shows the asymmetric shape and large sample-to-sample variations found in Monte-Carlo simulations and usually attributed to replica symmetry breaking. However, the scaling of the width of the distribution, and the link overlap in the presence of a weak coupling between the two replicas are in agreement with the droplet picture. We also discuss why it is impossible to see the asymptotic droplet-like behaviour for moderate system sizes and temperatures not too far below the critical temperature.

PACS. 75.50.Lk Spin glasses and other random magnets

1 Introduction

A series of computer simulations performed in the past few years [1,2] appear to support the claim that the three-dimensional Edwards-Anderson spin glass shows signatures of replica-symmetry breaking (RSB), implying the existence of infinitely many pure states in the low-temperature phase. In contrast, almost rigorous arguments [3] and a numerical analysis of the ground state structure [4] favour the droplet picture [5–7] with only one pair of pure states. Some recent experimental publications, *e.g.* [8], also favour the droplet picture, while others are less definite [9].

In a recent paper [10], we have suggested that due to the high temperatures and small system sizes the computer simulations [1,2] are strongly affected by the critical point and do not reflect the true low-temperature behaviour. This suggestion was supported by a numerical calculation of the Parisi overlap function using the Migdal-Kadanoff approximation (MKA). For the system sizes and temperatures typically used in computer simulations we found overlap functions similar to those in [1], however for lower temperatures we found agreement with the predictions of the droplet picture. That the results of computer simulations are strongly affected by the critical point can also be concluded from [11], where the Parisi overlap function shows critical scaling (with effective exponents) down to temperatures $\simeq 0.8T_{\rm c}$.

In recent publications [12–14], it is claimed that nontrivial behaviour of a quantity called the link overlap is a reliable indicator of RSB. However, in order to place such a claim on solid ground, one would have to show that the data cannot be interpreted within the framework of the droplet picture. It is the goal of this paper to furnish this discussion which has been missing so far. As in [10], we use the MKA which is known to agree with the droplet picture. Our results show, as in the case of the Parisi overlap function, that several nontrivial features attributed to RSB are in fact due to finite-size effects, and that the numerical data on the link overlap published so far are indeed in agreement with the droplet picture. We also derive expressions for the effective coupling at any temperature as a function of system size and find that one indeed needs rather large systems or low temperatures to see droplet-like behaviour.

The outline of this paper is as follows: After introducing the model and defining the quantities to be evaluated, we present first our analytical and numerical results for the link overlap distribution function. Then, we evaluate the link overlap in the presence of a weak coupling between the two replicas. In the following section we explain why finite size effects are so large for the three–dimensional Ising spin glass. Finally, we summarize and discuss our findings.

2 Definitions

The Hamiltonian H_0 of the Edwards-Anderson (EA) spin glass in the absence of an external magnetic field is given by

$$\beta H_0 = -\sum_{\langle i,j\rangle} J_{ij}\sigma_i\sigma_j,$$

where $\beta = 1/k_{\rm B}T$. The Ising spins can take the values ± 1, and the nearest-neighbour couplings J_{ij} are independent from each other and Gaussian distributed with a standard deviation J.

[a] e-mail: drossel@a13.ph.man.ac.uk

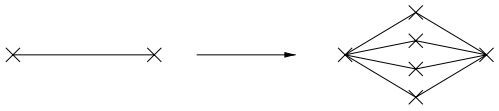

Fig. 1. Construction of a hierarchical lattice.

It has proven useful to consider two identical copies (replicas) of the system, and to measure overlaps between them. This gives information about the structure of the low-temperature phase, in particular about the number of pure states. The quantity considered in this paper is the link overlap

$$q^{(L)}(\epsilon) = (1/N_L) \sum_{\langle i,j \rangle} \langle \sigma_i \sigma_j \tau_i \tau_j \rangle \qquad (1)$$

where the sum is over all nearest-neighbour pairs $\langle i, j \rangle$ of a lattice with N_L bonds and N sites, and the brackets denote the thermal and disorder average. σ and τ denote the spins in the two replicas. The Hamiltonian used for the evaluation of the thermodynamic average is

$$\beta H[\sigma, \tau] = \beta H_0[\sigma] + \beta H_0[\tau] - \epsilon \sum_{\langle i,j \rangle} \sigma_i \sigma_j \tau_i \tau_j \,, \qquad (2)$$

where H_0 is the ordinary spin glass Hamiltonian given above, and the term in ϵ introduces a coupling between the two replicas.

In cases where the random couplings J_{ij} are taken to have the values ± 1, the link overlap is identical to the energy overlap. The main qualitative differences between the Parisi overlap

$$q^{(P)} = \sum_{i=1}^{N} (1/N) \langle \sigma_i \tau_i \rangle \,,$$

and the link overlap are (i) that flipping all spins in one of the two replicas changes the sign of $q^{(P)}$ but leaves $q^{(L)}$ invariant, and (ii) that flipping a droplet of finite size in one of the two replicas changes $q^{(P)}$ by an amount proportional to the volume of the droplet, and $q^{(L)}$ by an amount proportional to the surface of the droplet.

Below, we will show that, just as for the Parisi overlap, the MKA can reproduce all the essential features of the link overlap found in Monte-Carlo simulations. These results refute the claim made in [14] that the agreement between the MKA and simulations for the Parisi overlap reported in [10] is a mere coincidence that does not extend to the link overlap. The conclusion must be drawn that there is no evidence for RSB in three dimensional Ising spin glasses.

Evaluating a thermodynamic quantity in MKA in three dimensions is equivalent to evaluating it on a hierarchical lattice that is constructed iteratively by replacing each bond by eight bonds, as indicated in Figure 1. The total number of bonds after I iterations is 8^I, which is identical to the number of lattice sites of a three-dimensional lattice of size $L = 2^I$. Thermodynamic quantities are then evaluated iteratively by tracing over the spins on the highest level of the hierarchy, until the lowest level is reached and the trace over the remaining two spins is calculated [15]. This procedure generates new effective couplings, which have to be included in the recursion relations. In [16], it was proved that in the limit of infinitely many dimensions (and in an expansion away from infinite dimensions) the MKA reproduces the results of the droplet picture. We have shown in [10] that the MKA agrees with the droplet picture in three dimensions as well. For this reason, no feature that is seen in MKA can be attributed to RSB.

3 The probability distribution of the link overlap

We first set the coupling strength ϵ in equation (2) to zero and study the probability distribution $P(q^{(L)})$ of the link overlap, averaged over a sufficiently large number of samples. RSB should manifest itself in $P(q^{(L)})$ according to [12,13] in an asymmetric (non-Gaussian) shape and a nonzero width even at infinitely large system sizes. Furthermore, the link overlap for single samples should show large variations between different samples. Here, we show that the asymmetric shape and large sample to sample variations can even be seen in MKA for moderate system sizes and can therefore not be taken as evidence for RSB. The only reliable indicator for RSB would be a width of $P(q^{(L)})$ that does not shrink with increasing system size. However, the only Monte-Carlo simulation data published so far for $P(q^{(L)})$ [13] are taken for a four-dimensional Ising spin glass in a magnetic field, and they show a shrinking width, in agreement with the expectations from the droplet picture.

We have obtained the function $P(q^{(L)})$ by first calculating its Fourier transform,

$$F(y) = \left\langle \exp\left(\mathrm{i}y \sum_{\langle ij \rangle} \frac{\sigma_i \tau_i \sigma_j \tau_j}{N_L} \right) \right\rangle .$$

The coefficients a_n in

$$P(q^{(L)}) = \sum_{n=-N_L/2}^{N_L/2} a_n \delta(q^{(L)} - 2n/N_L)$$

are then found from $F(y)$:

$$a_n = (1/\pi N_L) \int_{-\pi N_L/2}^{\pi N_L/2} F(y) \exp(2\mathrm{i}yn/N_L) \mathrm{d}y.$$

Figures 2, 3 and 4 show our result for $P(q^{(L)})$ in MKA for three different temperatures. All curves have been averaged over several thousand samples. The curves for small L are asymmetric at $T = T_\mathrm{c}$ with a tail on the right-hand side. With decreasing temperature, the asymmetry becomes stronger, the tail moves to the left-hand side, and

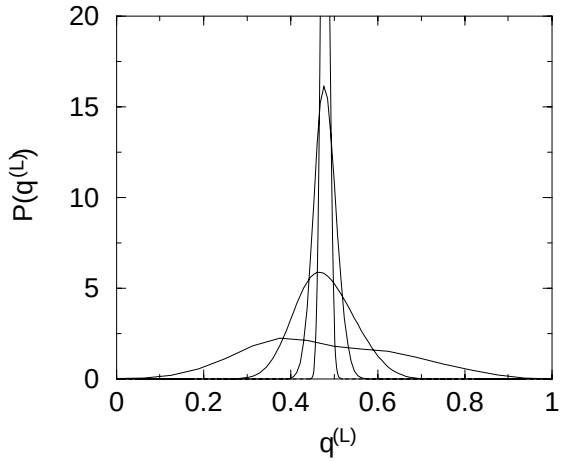

Fig. 2. The link overlap distribution $P(q^{(L)})$ for $T = T_c$ and $L = 4$, 8, 16, 32 (from widest to narrowest curve).

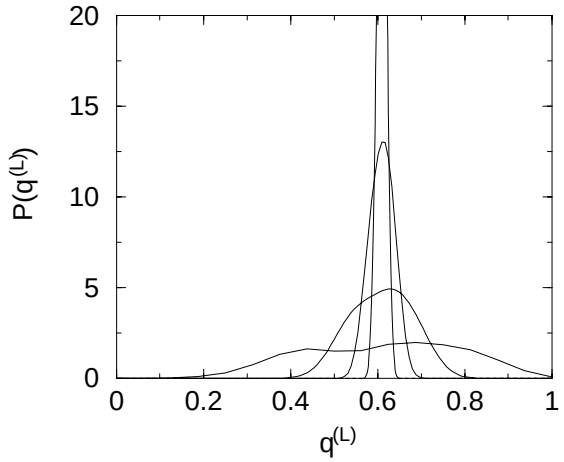

Fig. 3. The link overlap distribution $P(q^{(L)})$ for $T = 0.7T_c$ and $L = 4$, 8, 16, 32 (from widest to narrowest curve).

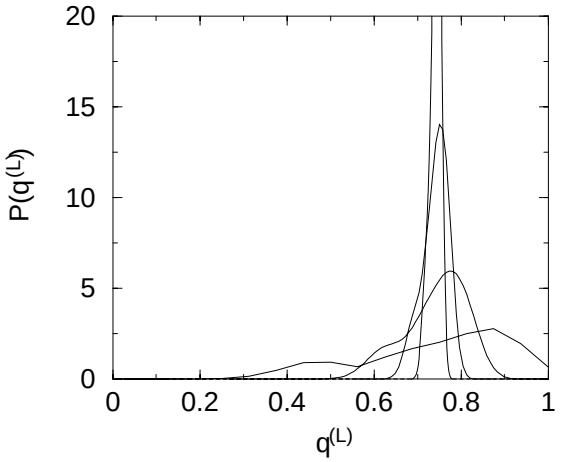

Fig. 4. The link overlap distribution $P(q^{(L)})$ for $T = 0.45T_c$ and $L = 4$, 8, 16, 32 (from widest to narrowest curve).

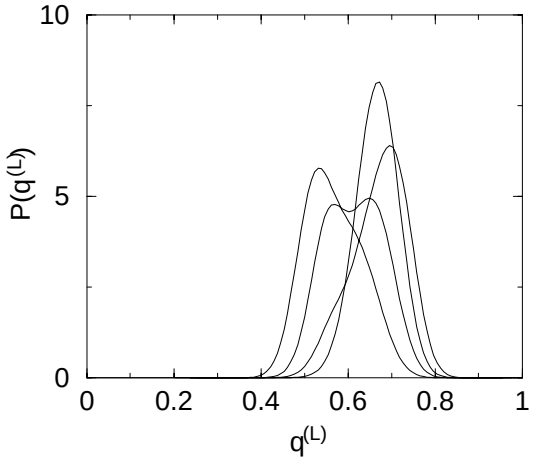

Fig. 5. The link overlap distribution $P(q^{(L)})$ for four different samples at $L = 8$ and $T = 0.7T_c$.

a shoulder is formed. All these features seem to be finite-size effects, as they become weaker with increasing system size.

Figures 5 and 6 show $P(q^{(L)})$ for single samples at $T = 0.7T_c$ and for $L = 8$ (Fig. 5) and $L = 16$ (Fig. 6). In particular for $L = 8$, there are large variations between different samples, a feature that is usually assumed to be a clear indicator of RSB. However, since the MKA does not show RSB, we must assign this feature to finite-size effects.

Finally, let us study the width

$$\Delta q^{(L)} = \sqrt{\int_{-1}^{1} (q^{(L)} - \bar{q}^{(L)})^2 P(q^{(L)}) \mathrm{d}q^{(L)}}$$

of $P(q^{(L)})$. Figure 7 shows our results on a double logarithmic plot, together with a power-law fit $q^{(L)} \sim L^{-\omega}$.

At $T = T_c$, the exponent ω is sufficiently close to $d/2 = 1.5$ to suggest that the leading contribution to $\Delta q^{(L)}$ comes from the superposition of independent contributions of the different parts of the system, just as it does for higher temperatures. Below, we shall see explicitly that critical point nonanalyticities are indeed subleading to the regular contributions.

Within the framework of the droplet picture, the value of ω at the zero temperature fixed point can be calculated as follows: The main excitations at low temperatures or large scales are droplets of flipped spins of a radius $r \simeq L$ in one of the replicas. Such droplets occur with a probability proportional to

$$(L/r)^d r^{-\theta} kT,$$

and each of them makes a contribution of the order

$$r^{2d_s} L^{-2d}$$

to $(\Delta q^{(L)})^2$. d_s is the fractal dimension of the droplet surface and is $d - 1$ in MKA, and θ is the scaling exponent of the coupling strength and has a value around 0.24 in MKA in $d = 3$. We therefore find

$$\Delta q^{(L)} \sim \sqrt{kT} L^{d_s - d - \theta/2},$$

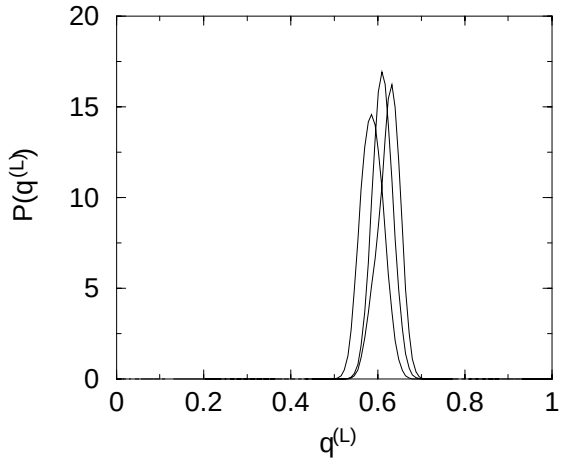

Fig. 6. The link overlap distribution $P(q^{(L)})$ for three different samples at $L = 16$ and $T = 0.7T_c$.

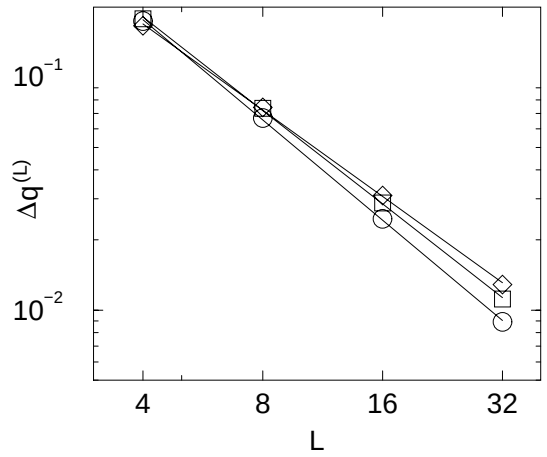

Fig. 7. Width of $P(q^{(L)})$, $\Delta q^{(L)}$, as a function of L for $T = T_c$ (circles), $T = 0.7T_c$ (squares) and $T = 0.45T_c$ (diamonds), together with a power-law fit. The exponents of the three fits are 1.43, 1.33 and 1.23.

giving $\omega \simeq 1.12$ in MKA. Our above data for $T = 0.45T_c$ are not far from this result. For larger system size, they must ultimately converge to it. Just as in the case of the Parisi overlap [10], the crossover from critical to low-temperature behaviour is so slow that even for $T \simeq 0.4T_c$ the asymptotic regime is not reached for system sizes up to 32, and the curves appear to show effective exponents.

For a cubic lattice, we have $d_s \simeq 2.2$ [17] and $\theta \simeq 0.2$ [5,18], predicting a value $\omega \simeq 0.9$ within the framework of the droplet picture. However, very recent data [4] suggest that d_s might in fact be as large as 2.7, which would lead to $\omega \simeq 0.4$. This has to be compared to the RSB scenario, where $\omega = 0$. In [14], it is claimed that Monte-Carlo simulation data at $T \simeq 0.6T_c$ and $L \leq 12$ show already the signatures of RSB. However, as yet there is no published data for $\Delta q^{(L)}$. Only if the value of ω drops below the value predicted by the droplet picture and approaches zero with increasing system size, can one conclude that RSB occurs. (The fact that $P(q^{(L)})$ changes its shape with increasing system size may lead to additional delays in reaching the asymptotic large L limit.)

4 The link overlap in the presence of a coupling between the two replicas

In [12,14], the authors suggested studying the expectation value of the link overlap in the presence of a coupling between the two replicas, $q^{(L)}(\epsilon)$, in order to test whether a system shows RSB. A positive coupling ϵ in equation (2) favours a configuration where both replicas are in the same state, while a negative ϵ favours configurations with smaller overlaps. If the RSB scenario were correct, the distribution $P(q^{(L)})$ would have a finite width even for $L \to \infty$ and range from some minimum value $q_{\min}$ to a maximum value $q_{\max}$. Consequently, the expectation value of the link overlap, $q^{(L)}(\epsilon)$, would have a jump from $q_{\min}$ to $q_{\max}$ at $\epsilon = 0$ in the thermodynamic limit $L \to \infty$ [14]. In contrast, as we will show next, the droplet picture predicts a continuous and at $\epsilon = 0$ nonanalytic function $q^{(L)}(\epsilon)$ [19]. Part of these results were published in [19].

Within the droplet picture, the scaling dimension of ϵ in the spin glass phase can easily be obtained. At length scale 1, ϵ is equivalent to the energy cost of flipping one spin in one of the two replicas. On a scale l, this becomes the energy cost of flipping a droplet of radius l in one of the replicas, which is proportional to ϵl^{d_s}. The scaling dimension of ϵ is therefore d_s, where d_s is the fractal dimension of the droplet surface. Equivalently, d_s is the fractal dimension of a domain wall. Within MKA, we have $d_s = d - 1$. The same value $d - 1$ for the scaling dimension of ϵ is also obtained from an analytical calculation of the recursion relations for ϵ and the strength J of the random couplings near the $T = 0$ fixed point.

The positive dimension of ϵ implies that the coupling between the two replicas is a relevant perturbation and that on large scales a behaviour different from that of an independent system can be seen. When ϵ is positive, the energy cost ϵl^{d_s} for the excitation of droplets of radius l leads to the suppression of droplets larger than

$$l^* \sim (kT/\epsilon)^{1/d_s}.$$

On scales beyond l^*, droplet excitations must occur in both replicas simultaneously. This costs twice the energy of a single droplet in an independent system. The coupled system thus behaves on large scales exactly like a single system with twice the coupling strength J.

As stated in the preceding section, for $\epsilon = 0$ droplets of size l occur with a probability proportional to $(L/l)^d l^{-\theta} kT$ in a system of size L. Since for positive ϵ droplets of size greater than l^* are suppressed, the change in the link overlap due to a small positive ϵ can be written as

$$q^{(L)}(\epsilon) - q^{(L)}(0) \sim kT \sum_{l>l^*}^{L} l^{d_s - d - \theta}. \qquad (3)$$

In order to suppress each droplet only once, the sum must be taken over distinct length scales l, *e.g.*, $l = l^*, 2l^*, 4l^*, ...$, and it is proportional to the first term. Therefore, we can write $q^{(L)}(\epsilon) - q^{(L)}(0) \sim kT(l^*)^{d_s-d-\theta}$, and using the expression for l^* given above we have,

$$q^{(L)}(\epsilon) - q^{(L)}(0) \sim kT(\epsilon/kT)^{(d+\theta-d_s)/d_s}. \quad (4)$$

For negative ϵ, flipping a droplet of radius l in one of the replicas changes the system's energy by an amount proportional to $l^\theta - |\epsilon| l^{d_s}$, which is negative for $l > l_c$ with $l_c \sim |\epsilon|^{1/(\theta-d_s)}$. Therefore, there is a proliferation of droplets beyond this length scale and the spin glass state is completely restructured. We followed the flow of the parameters ϵ, J, and $\Delta\epsilon$ (the width of the distribution of ϵ) under a change of scale in the MKA and found that $\Delta\epsilon$ diverges, while J and ϵ eventually decrease to zero. Such a system is an Edwards-Anderson spin glass with the effective spins $\rho_i = \sigma_i\tau_i$.

Since droplets of size larger than l_c proliferate for negative ϵ, the change in the link overlap is given in this case by

$$q^{(L)}(\epsilon) - q^{(L)}(0) \sim -(l_c)^{d_s-d} \sim -|\epsilon|^{(d-d_s)/(d_s-\theta)}. \quad (5)$$

We thus find that $q^{(L)}(\epsilon) - q^{(L)}(0)$ has the form $A_\pm|\epsilon|^{\lambda_\pm}$, with values A and λ that depend on the sign of ϵ. Within MKA, it is $\lambda_+ \simeq 0.62$, and $\lambda_- \simeq 0.57$. For a cubic lattice, and with $d_s \simeq 2.2$ [17], one obtains $\lambda_+ \simeq 0.45$, and $\lambda_- \simeq 0.40$. Again, with the more recent value for d_s given in [4], we would get $\lambda_+ \simeq 0.19$, and $\lambda_- \simeq 0.13$.

For finite temperatures and small systems, there are corrections to this asymptotic behaviour due to finite-size effects which replace the nonanalyticity at $\epsilon = 0$ with a linear behaviour for small $|\epsilon|$, and due to the influence of the critical fixed point, where the leading behaviour is linear in ϵ (see below). As we have argued in [10], the influence of the critical fixed point changes the apparent value of the low-temperature exponents for the system sizes studied in Monte-Carlo simulations and the MKA. The data shown in [14] with an apparent value of 0.5 for $\lambda_\pm$ are fully compatible with the above predictions of the droplet picture. There is no indication of a jump at $\epsilon = 0$ in $q^{(L)}(\epsilon)$, which would be the signature of RSB. For the MKA, the apparent exponent at $0.7T_c$ is close to 1 for $L \simeq 16$, leading to the "trivial" behaviour found in [14]. However, at lower temperatures, for the same small system sizes the above-mentioned nontrivial features predicted by the droplet picture become clearly visible, as shown in Figure 8.

Let us conclude this section with a discussion of the link overlap at the critical temperature. Figure 9 shows our result in MKA. Clearly, the curves are linear at $\epsilon = 0$, indicating that the regular part dominates over the singular, critical contribution. This conclusion is confirmed by studying the scaling dimension of ϵ at T_c. Iterating the recursion relations for the coupling constants, we find that under a change in length scale, $x \to x/b$, we obtain $\epsilon \to b^\phi\epsilon$ with $\phi \simeq 1.14$. Now, $q^{(L)}(\epsilon)$ can be obtained from the free energy *via* the relation

$$q^{(L)}(\epsilon) = (1/3N)\partial(\ln Z)/\partial\epsilon,$$

implying a scaling behaviour $q^{(L)} \to b^{d-\phi}q^{(L)}$. Substituting b with ϵ gives then the relation

$$q^{(L)} \sim \epsilon^{(d-\phi)/\phi} \simeq \epsilon^{1.6}.$$

Compared to the linear regular part, this singular dependence cannot be seen for small ϵ.

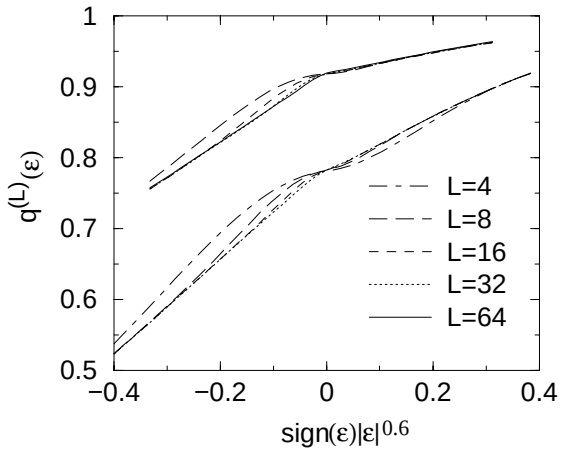

Fig. 8. $q^{(L)}(\epsilon)$ in MKA at $T \simeq 0.38T_c$ (bottom) and $0.14T_c$ (top) as function of $\mathrm{sign}(\epsilon)|\epsilon|^{0.6}$ for various system sizes. Each curve is averaged over several 1000 samples.

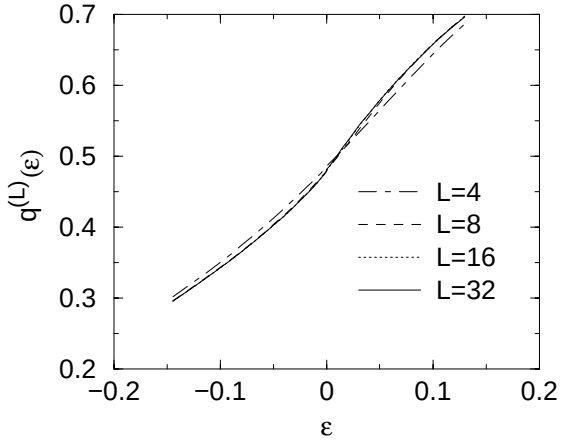

Fig. 9. $q^{(L)}(\epsilon)$ in MKA at $T \simeq T_c$ for various system sizes.

5 Finite size effects

As we have argued throughout this paper and in earlier work [10,19], finite size effects appear to be large for the Ising spin glass in three dimensions. To understand this behaviour, we iterated the MK recursion relations starting at various temperatures below T_c. In Figure 10 the solid lines show the data for J_n^2 as a function $L = 2^n$ where n is the number of iterations of the MK recursion relations. For large L, one expects $J_n^2 \simeq 2^{2n\theta}$. However, it is

apparent that even at $T \simeq 0.7T_c$ one needs system sizes $L \simeq 100$ to see this behaviour. Because the change in the slope $\mathrm{d}\ln J^2/\mathrm{d}\ln L$ is so slow, $J^2(L)$ appears to be described by a power law with some effective exponent over small windows of one decade in L, just as we found for $P^{(P)}(0)$ in [10]. To understand the large crossover regime, we consider an expansion around the zero-temperature fixed point, where the effective temperature $T = 1/J$ at a length scale L can be written as

$$\mathrm{d}T/\mathrm{d}\ln L = -\theta T + AT^3 + BT^5 + ..., \qquad (6)$$

where A, B, ... are constants and even order terms are absent because $T \to -T$ (or $\{J_{ij}\} \to \{-J_{ij}\}$) is a symmetry of the Hamiltonian. Now, $d = 3$ is close to the lower critical dimension for Ising spin glasses (so that T_c is in some sense small), and one might expect that truncating the above equation after the first few terms will give a good approximation for T or equivalently J throughout the low temperature phase. We now show that this is indeed the case: keeping terms up to T^5 gives a good description of the MK data of Figure 10.

The analysis is as follows: At T_c, $\mathrm{d}T/\mathrm{d}L = 0$ so that $\theta = AT_c^2 + BT_c{}^4$. For small deviations away from T_c *i.e.* $T = T_c + \delta T$, the correlation length exponent ν is defined *via* $\mathrm{d}\ln(\delta T)/\mathrm{d}\ln L = 1/\nu$, leading to $1/\nu = 2\theta + 2BT_c^4$. Solving for A and B in terms of ν, θ and T_c, we find $A = (2\theta - 1/2\nu)/T_c^2$ and $B = (1/\nu - 2\theta)/2T_c^4$. Now we substitute these expressions into the above equation and integrate from a length scale L_0 (temperature T_0) to a length scale L (temperature T_L) to get an equation relating T_L to T_0. Then using $T_L = 1/J_L$ gives the corresponding equation for J_L. Setting $L/L_0 = 2^n$ and $2\theta\nu = x$, we find

$$\frac{(J_n^2 - J_c^2)^x}{\left[J_n^2 - \frac{x-1}{x}J_c^2\right]^{(x-1)}} = \frac{(J_0^2 - J_c^2)^x}{\left[J_0^2 - \frac{x-1}{x}J_c^2\right]^{(x-1)}} 2^{2n\theta}, \qquad (7)$$

where J_0 is the coupling at the starting point $n = 0$ and J_n is the coupling after n iterations.

To test whether equation (7) is a good approximation, we have inserted the values J_n^2 obtained from the MK recursion relations into the left hand side of equation (7). We have chosen $\nu = 2.8$ and $\theta = 0.25$, in agreement with [10,15]. The result are the data points given in Figure 10. They satisfy a power law with exponent 2θ and a prefactor $(J_0^2 - J_c^2)^x/(J_0^2 - (x - 1/x)J_c^2)^{(x-1)}$, showing that equation (7) is indeed an appropriate description of the growth of the coupling throughout the low temperature phase. Now, for large J_n and J_0, equation (7) reduces to pure power law behaviour viz. $J_n^2 \simeq J_0^2 2^{2n\theta}$ and the crossover length for the different temperatures can be read off as the length for which $(J_n^2 - J_c^2)^{2\theta\nu}/(J_n^2 - (2\theta\nu - 1)J_c^2/2\theta\nu)^{(2\theta\nu-1)}$ becomes of the same order as J_n^2. Beyond the crossover length, we should see the correct low-temperature exponents.

Thus, we have seen that the three-dimensional spin glass in MKA can be well described by an approximation that is valid close to the lower critical dimension and that shows explicitly that crossover scales are large. The analysis described above is quite general and should be applicable also to the Ising spin glass on a cubic lattice. There is one caveat however: the analysis we have carried out is valid for the couplings alone. Other quantities (for example $P(q^{(P)})$ or $P(q^{(L)})$) would have to be studied separately and it is possible that the crossover lengths would be somewhat different for different quantities.

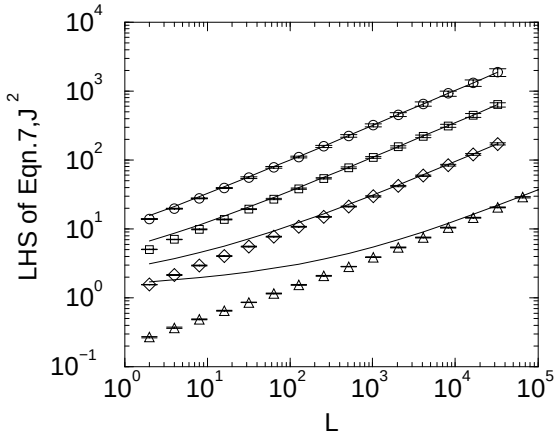

Fig. 10. J_n^2 (solid lines) and left hand side of equation (7) (symbols) as a function of system size $L = 2^n$ for (from top to bottom) $T = 0.3T_c$, $0.5T_c$, $0.7T_c$, $0.9T_c$.

6 Conclusion

In this paper, we have studied the link overlap between two identical replicas of a three-dimensional Ising spin glass in Migdal-Kadanoff approximation. The width of the link overlap distribution decreases to zero with increasing system size at T_c as well as in the low-temperature phase. These findings are in agreement with the predictions of the droplet picture. For system sizes similar to the ones used in Monte-Carlo simulations of a cubic lattice, we find the same large sample-to-sample fluctuations and asymmetric curve shapes as reported from those simulations. They must be interpreted as a finite-size effect and cannot be taken as an indicator for replica-symmetry breaking. The only reliable indicator for RSB would be a width of the overlap distribution that does not decrease with increasing system size.

Similarly, the link overlap in the presence of a weak coupling between the two replicas shows in MKA in the spin glass phase the singular behaviour predicted by the droplet picture. Data from Monte-Carlo simulations are also in full agreement with the droplet picture. The RSB picture predicts a jump in the mean value of the link overlap at zero coupling strength that is not visible in Monte-Carlo simulation data published so far.

We have reproduced phenomenologically the influence of the critical point on the growth of the coupling constants using an approximation that is valid close to the lower critical dimension. This gives us a direct estimate of the lengthscale at any given temperature beyond which one needs to go in order to see zero-temperature (droplet)

scaling without crossover effects from critical point behaviour intruding too strongly. This crossover effect often seems to get overlooked in the literature. For example Komori, Yoshino and Takayama [20] in a numerical simulation of the Ising spin glass at a temperature of $0.84T_c$ found that critical scaling of the dynamics worked well: they found that correlation data at time t could be collapsed for systems of linear dimension L for values of L up to 7, by plotting against the variable $t/L^{z(T)}$, where $z(T)$ is similar to the critical point dynamical exponent. This behaviour was interpreted by Marinari, Parisi and Ruiz-Lorenzo [21] as evidence against droplet scaling but it is clear from our work that for the system sizes studied at temperatures so close to T_c droplet scaling would be unobservable and that critical point scaling should indeed work quite well.

We therefore conclude that the droplet picture, combined with finite-size effects, can fully explain all data for the link overlap in the Ising spin glass. There is no evidence for the presence of RSB.

We benefitted from discussions with E. Marinari. This work was supported by EPSRC Grants GR/K79307 and GR/L38578.

References

1. E. Marinari, G. Parisi, J.J. Ruiz-Lorenzo, Phys. Rev. B **58**, 14852 (1998).
2. E. Marinari, G. Parisi, F. Ricci-Tersenghi, J.J. Ruiz-Lorenzo, J. Phys. A **31**, L481 (1998).
3. C.M. Newman, D.L. Stein, Phys. Rev. E **57**, 1356 (1998).
4. M. Palassini, A.P. Young, preprint `cond-mat/9906323`.
5. W.L. McMillan, J. Phys. C **17**, 3179 (1984).
6. D.S. Fisher, D.A. Huse, Phys. Rev. Lett. **56**, 1601 (1986).
7. A.J. Bray, M.A. Moore, in *Heidelberg Colloquium in Glassy Dynamics*, edited by J.L. van Hemmen, I. Morgenstern, *Lecture Notes in Physics*, Vol. 275 (Springer-Verlag, Heidelberg, 1987).
8. T. Jonsson, K. Jonason, P. Nordblad, Phys. Rev. B **59**, 9402 (1999).
9. K. Jonason, E. Vincent, J. Hammann, J.-P. Bouchaud, P. Nordblad, Phys. Rev. Lett. **81**, 3243 (1998).
10. M.A. Moore, H. Bokil, B. Drossel, Phys. Rev. Lett. **81**, 4252 (1998).
11. B.A. Berg, W. Janke, Phys. Rev. Lett. **80**, 4771 (1998).
12. E. Marinari, G. Parisi, J.J. Ruiz-Lorenzo, in *Spin Glasses and Random Fields*, edited by P. Young (World Scientific 1998).
13. E. Marinari, C. Naitza, F. Zuliani, J. Phys. A **31**, 6355 (1998).
14. E. Marinari, G. Parisi, J.J. Ruiz-Lorenzo, F. Zuliani, Phys. Rev. Lett. **82**, 5176 (1999).
15. B.W. Southern, A.P. Young, J. Phys. C **10**, 2179 (1977).
16. E. Gardner, J. Phys. France **45**, 1755 (1984).
17. D.A. Huse, Phys. Rev. B **43**, 8673 (1991).
18. A.J. Bray, M.A. Moore, J. Phys. C **17**, 476 (1984).
19. H. Bokil, A. Bray, B. Drossel, M.A. Moore, Phys. Rev. Lett. **82**, 5177 (1999).
20. T. Komori, H. Yoshini, H. Takayama, J. Phys. Soc. Jpn **68**, 3387 (1999).
21. E. Marinari, G. Parisi, J.J. Ruiz-Lorenzo, `cond-mat/9904321`.